

A SHAPIRO DELAY DETECTION IN THE BINARY SYSTEM HOSTING THE MILLISECOND PULSAR PSR J1910–5959A

A. CORONGIU¹, M. BURGAY¹, A. POSSENTI¹, F. CAMILO², N. D'AMICO^{1,3}, A. G. LYNE⁴, R. N. MANCHESTER⁵, J. M. SARKISSIAN⁶, M. BAILES⁷, S. JOHNSTON⁵, M. KRAMER^{4,8}, AND W. VAN STRATEN⁷

¹ INAF-Osservatorio Astronomico di Cagliari, Loc. Poggio dei Pini, Strada 54, I-09012 Capoterra (CA), Italy

² Columbia Astrophysics Laboratory, Columbia University, 550 West, 120th Street, New York, NY 10027, USA

³ Università degli Studi di Cagliari, Dip. di Fisica, S.S. Monserrato-Sestu km 0,700, I-09042 Monserrato (CA), Italy

⁴ Jodrell Bank Centre for Astrophysics, School of Physics and Astronomy, University of Manchester, Manchester M13 9PL, UK

⁵ CSIRO Astronomy and Space Science, Australia Telescope National Facility, P.O. Box 76, Epping, NSW 1710, Australia

⁶ Australia Telescope National Facility, CSIRO, Parkes Observatory, P.O. Box 276, Parkes, NSW 2870, Australia

⁷ Centre for Astrophysics and Supercomputing, Swinburne University of Technology, P.O. Box 218 Hawthorn, VIC 3122, Australia

⁸ Max-Planck-Institut für Radioastronomie, Auf dem Hügel 69, D-53121 Bonn, Germany

Received 2012 June 27; accepted 2012 October 2; published 2012 November 8

ABSTRACT

PSR J1910–5959A is a binary pulsar with a helium white dwarf (HeWD) companion located about 6 arcmin from the center of the globular cluster NGC 6752. Based on 12 years of observations at the Parkes radio telescope, the relativistic Shapiro delay has been detected in this system. We obtain a companion mass $M_C = 0.180 \pm 0.018 M_\odot$ (1σ) implying that the pulsar mass lies in the range $1.1 M_\odot \leq M_P \leq 1.5 M_\odot$. We compare our results with previous optical determinations of the companion mass and examine prospects for using this new measurement for calibrating the mass–radius relation for HeWDs and for investigating their evolution in a pulsar binary system. Finally, we examine the set of binary systems hosting a millisecond pulsar and a low-mass HeWD for which the mass of both stars has been measured. We confirm that the correlation between the companion mass and the orbital period predicted by Tauris & Savonije reproduces the observed values but find that the predicted $M_P - P_B$ correlation overestimates the neutron star mass by about $0.5 M_\odot$ in the orbital period range covered by the observations. Moreover, a few systems do not obey the observed $M_P - P_B$ correlation. We discuss these results in the framework of the mechanisms that inhibit the accretion of matter by a neutron star during its evolution in a low-mass X-ray binary.

Key words: globular clusters: individual (NGC 6752) – pulsars: individual (PSR J1910–5959A)

1. INTRODUCTION

PSR J1910–5959A (henceforth PSRA) is a millisecond pulsar (MSP) discovered in the Parkes Globular Cluster Pulsar Survey (D'Amico et al. 2001, hereafter Paper I). It has a spin period of 3.27 ms, and it orbits around a low-mass companion with $M_C \geq 0.2 M_\odot$, assuming a pulsar mass $M_P = 1.4 M_\odot$, with an orbital period $P_B = 0.84$ days. Because of its unusual position with respect to the core of the globular cluster NGC 6752 (its angular distance from the cluster center is $\theta_\perp = 6.4'$, corresponding to 3.3 half-mass radii; Paper I), it has been questioned whether this object is a member of the cluster (Bassa et al. 2006). In fact, of all cluster-associated MSPs, PSRA has the largest angular distance from the core of the hosting cluster.⁹

The binary companion of PSRA has been recognized as a helium white dwarf (HeWD) star by Ferraro et al. (2003) and independently by Bassa et al. (2003), via observations taken with the ESO Very Large Telescope and the *Hubble Space Telescope* (HST). The values obtained by these authors for the mass of the binary companion of PSRA are in agreement ($M_{co} \simeq 0.17\text{--}0.20 M_\odot$). Both authors also agree in concluding that the photometric properties of this star are consistent with the hypothesis that PSRA is associated with the globular cluster NGC 6752.

⁹ Intriguingly PSR J1910–5959C in the same cluster ranks second in this list, and is located at $\theta_\perp = 2.7'$, corresponding to 1.4 half-mass radii from the core of the cluster (Paper I).

The radial velocity curve of the companion of PSRA has been investigated by Cocozza et al. (2006) and Bassa et al. (2006) through phase-resolved spectroscopy in the optical band with HST observations. The resulting values for the mass ratio of the binary system for the mass of the optical companion and the orbital inclination were also compatible with each other, although Bassa et al. (2006) obtained more stringent constraints (see Section 3.2 for details). Bassa et al. (2006) carefully discussed the association of this binary system with NGC 6752 and indicated a preference for non-association, though their arguments are not conclusive because of the large uncertainties on the parameters that would allow one to discriminate between the two scenarios (see Section 3.2 for details).

A refined ephemeris for PSRA was presented by Corongiu et al. (2006, hereafter Paper II), where a low eccentricity model was applied to describe the pulsar's orbit. The measured eccentricity was $e \sim 3 \times 10^{-6}$ at a longitude of periastron $\omega \sim 90^\circ$. Paper II discussed the possibility that such eccentricity was indeed a misinterpreted Shapiro delay. Nevertheless, Paper II maintained a conservative approach to this problem and deferred the revision of this issue until a significantly longer time span of timing data became available.

Correlations between the orbital period, the pulsar mass, and the companion mass have been obtained by Tauris & Savonije (1999, hereafter TS99) from their numerical calculations on the non-conservative evolution of close binary systems with low-mass donor stars ($M_D < 2 M_\odot$), a $1.3 M_\odot$ accreting neutron star, and an orbital period $P_B \geq 2$ days at the beginning of their low-mass X-ray binary (LMXB) phase. These systems

have diverging orbital separation and are the progenitors of low-mass binary millisecond pulsars (Bhattacharya & van den Heuvel 1991). [TS99](#) obtained a positive correlation between the orbital period and the companion mass and a negative correlation between the orbital period and the pulsar mass. The predicted $M_C - P_B$ correlation has been observed by van Kerkwijk et al. (2005) and Lorimer (2008). [TS99](#) remarked on the discrepancy between the predicted $M_P - P_B$ correlation and the available data. However, in most cases the determinations of the M_C and M_P were based on models for the companion atmosphere or on statistical hypothesis for the orbital inclination, often leading to large uncertainties. The observation of a Shapiro delay allows one to obtain a direct measurement of M_C and M_P and gives a strong test for the aforementioned correlations.

In this paper, we present timing data for PSRA collected over 12 years at the Parkes radio telescope. This data span is twice than that used in [Paper II](#) and allowed us to get better constraints on the rotational, positional, and orbital parameters for PSRA, and to detect the Shapiro delay in this system. The paper is organized as follows. In Section 2, we briefly describe the observing methods and present the timing solution based on the available data span; in Section 3, we describe the method for measuring the Shapiro delay, present our determination of the companion mass, and discuss our results and their implications. In Section 4, we summarize the measurements for the masses of MSPs and their HeWD companions, focusing on those binaries for which M_C and M_P have been obtained from the detection of the Shapiro delay effect. We then compare these data to the predictions of [TS99](#) and discuss the results. In Section 5, we briefly summarize our work.

2. OBSERVATIONS AND GENERAL TIMING RESULTS

Regular pulsar timing observations of PSRA in NGC 6752 have been carried out since 2000 September with the Parkes 64 m radio telescope at a central frequency of 1390 MHz, using the central beam of the 20 cm multibeam receiver (Staveley-Smith et al. 1996) or the H-OH receiver. The hardware system is the same as that used in the discovery observations ([Paper I](#)). The effects of interstellar dispersion are minimized by using a filterbank having 512×0.5 MHz frequency channels for each polarization. After detection, the signals from individual channels are added in polarization pairs, integrated, 1-bit digitized every $80 \mu\text{s}$ ($125 \mu\text{s}$ in earlier observations), and recorded to magnetic tape for offline analysis. We synchronously folded the data at the pulsar period using the program DSPSR (van Straten & Bailes 2011) with a subintegration time of 1 minute and dedispersion in groups of 64 channels to give 8 frequency sub-bands. We visually inspected each file to extract the maximum number of pulse times of arrivals (ToAs), depending on integration time and interstellar scintillation which causes large fluctuations in the detected flux density. We considered a ToA reliable if the pulse profile had a signal-to-noise ratio greater than 5 and the pulse was visible. This approach gave us ~ 1000 ToAs at different frequencies within the band of the receivers and consequently allowed us to fit for the dispersion measure and its first derivative. We calculated the ToAs by fitting a template profile to the observed mean pulse profiles and we analyzed them using the program TEMPO2 (Hobbs et al. 2006) with the DE405 solar system ephemeris and the TT(TAI) reference timescale. Table 1 summarizes the best-fit values and 1σ uncertainties from TEMPO2 (everywhere in the paper all reported measures are quoted with their 1σ uncertainty, and all reported ranges are at the same confidence level). The timing residuals for the fit

Table 1
Measured and Derived Parameters for PSR J1910–5959A

Parameter	PSR J1910–5959A
R.A. (J2000)	19:11:42.75562(3)
Decl. (J2000)	−59:58:26.9029(3)
$\mu_\alpha \cos \delta$ (mas yr ^{−1})	−3.08(6)
μ_δ (mas yr ^{−1})	−3.97(6)
P (ms)	3.26618657079054(9)
\dot{P} (10^{-21})	2.94703(14)
DM (pc cm ^{−3})	33.6998(16)
DM1 (pc cm ^{−3} s ^{−1})	0.00136(36)
Binary model	DD
P_{orb} (days)	0.83711347691(3)
$a_P \sin i$ (lt-s)	1.2060418(7)
T_0 (MJD)	51919.206480057(55)
$M_c^{(a)}$ (M_\odot)	0.180(18)
$\sin i^{(a)}$	≥ 0.9994
$i^{(a)}$ (deg)	$\geq 88^\circ$
$f(M_{\text{PSR}})(M_\odot)$	0.00268782589(5)
μ (mas yr ^{−1})	5.02(6)
Position angle (deg)	217.9(7)
Ref. Epoch (MJD)	51920.000
MJD range	51710–55911
Number of TOAs	1003
Rms residuals (μs)	5.3

Notes. Units of right ascension are hours, minutes, and seconds, and units of declination are degrees, arcminutes, and arcseconds. Numbers enclosed in parenthesis represent the 1σ uncertainties on the last significant digit for all parameters, either measured and derived, presented in this table. The values and relative uncertainties for the parameters that describe the Shapiro delay (indicated with the apex *a*) have been obtained through a Bayesian analysis of our timing results. The proper motion's position angle is measured counterclockwise starting from the north direction.

which have a χ^2 of 989.3 (with 989 degrees of freedom) are shown in Figure 1, against MJD in the upper panel and against orbital phase in the lower panel. We determined the values and the uncertainties for the Shapiro delay parameters through a Bayesian analysis (see Section 3).

The new positional and rotational parameters at the reference epoch are all consistent with those reported in [Paper I](#) and [Paper II](#) at a confidence level of 2σ , with the only exception being the proper motion, whose components in right ascension and declination are consistent at the 4σ and 6σ levels, respectively. The value for the first derivative of the dispersion measure (DM1) is of the same order of magnitude of similar determinations for other MSPs. The consistency of the orbital parameters will be discussed in Section 3.

3. THE SHAPIRO DELAY MEASUREMENT

3.1. Method

The orbital solutions presented and discussed in [Papers I](#) and [II](#) were based on the ELL1 binary model, which is suitable for systems with small orbital eccentricities (N. Wex 1998 unpublished work; see Lange et al. 2001). In [Paper II](#), an orbital eccentricity $e = (3.4 \pm 0.6) \times 10^{-6}$ was reported at a longitude of periastron $\omega = 90^\circ \pm 10^\circ$. The values obtained for e and in particular for ω were already commented as a possible misinterpretation of a Shapiro delay ([Paper II](#)). By applying the same binary model of [Paper II](#) to the longer data span presented in this work, we obtain $e = (3.5 \pm 0.5) \times 10^{-6}$ at a longitude of

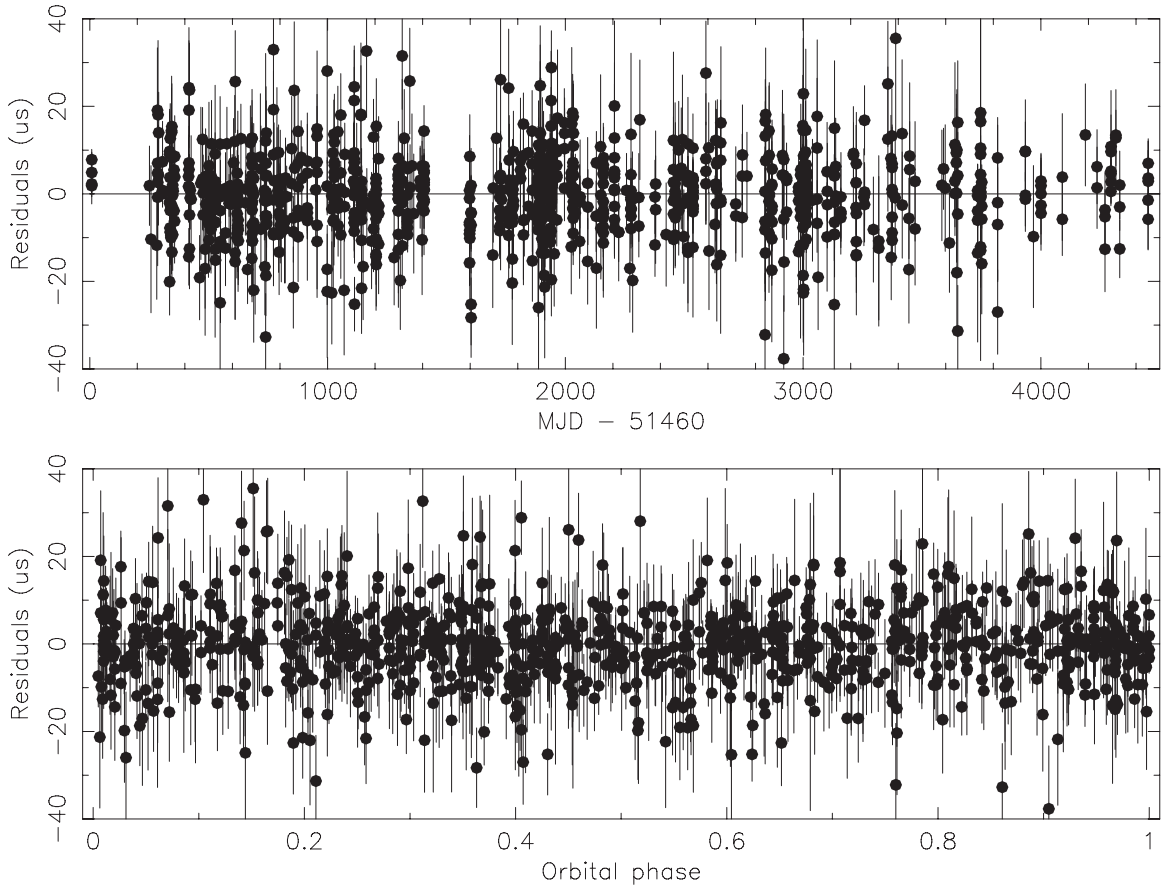


Figure 1. Timing residuals vs. Modified Julian Date (MJD, upper panel) and orbital phase (lower panel) for the timing solution presented in this work.

periastron $\omega = 95^\circ \pm 7^\circ$. Since the uncertainties on these two parameters did not decrease as expected for the case of a pure Keplerian ELL1 model, we carefully reinvestigated the possible presence of a Shapiro Delay.

We used the DD binary model (Damour & Deruelle 1985, 1986) and included the two parameters that describe the Shapiro delay, namely, the range r and the shape s . These two parameters are directly related to the companion mass M_C and the orbital inclination i through the simple relations $r = T_\odot M_C / (GM_\odot/c^3)$, where G is Newton's universal gravitation constant and c is the speed of light) and $s = \sin i$ (see, e.g., Lorimer & Kramer 2004). Figure 2 displays our attempts to detect the first and third harmonics of the Shapiro delay in our timing residuals. We recall (e.g., Lorimer & Kramer 2004) that the first harmonic is obtained by fitting for all parameters, including the ones describing the Shapiro delay, then resetting $M_C = 0.0$ and $\sin i = 1.0$ while keeping all other parameters to their best-fit values, and finally by plotting the resulting timing residuals. The third harmonic is obtained by fitting for all parameters but the Shapiro delay ones, which remain set to the values $M_C = 0.0$ and $\sin i = 1.0$, then plotting the residuals for this best-fit solution obtained in this way. While the first harmonic is still consistent with the response for an elliptic orbit, the third harmonic is a unique signature of the Shapiro delay. In the upper panels of Figure 2, timing residuals show some evidence of the harmonic structure, while in lower panels, where residuals have been rebinned in 20 orbital phase bins, the two harmonics are clearly recognizable. As a further comparison, in the lower panels we plot (solid lines) the theoretical curves for the Shapiro delay with which our rebinned residuals are in satisfactory agreement.

As an additional sanity check, we have checked the consistency of the three Keplerian parameters that are common to the two different orbital models presented in Paper II and in this work. The values for P_B are fully consistent to each other, and the same is true comparing T_{ASC} in Paper II and T_0 here. We recall that in the case of zero eccentricity orbits, the periastron is defined as coincident to the ascending node. The only parameter for which we now find an inconsistency at a level of about 10σ with respect to Paper II is the orbit projected semimajor axis $a_P \sin i$. However, because of the change in the adopted binary model (from ELL1 to DD), this parameter cannot be directly compared. The quantity to be compared between is $a_P \sin i / (1 + e)$. From Paper II, we obtain $a_P \sin i / (1 + e) = 1.2060425 \pm 0.0000007$, while in this work it results $a_P \sin i = 1.2060420 \pm 0.0000008$, as the orbital eccentricity has been now set to zero. The two values are then in full agreement.

We obtained the values for the companion mass and the inclination angle through a Bayesian analysis on our timing residuals. The method is described in Splaver et al. (2002). We chose the a priori probability density functions as follows.

1. A flat distribution for $\cos i$ in the range $0 \leq \cos i \leq 1$, as we assumed a randomly oriented orbit in space.
2. A flat distribution for M_C in the range $0.0 M_\odot \leq M_C \leq 0.5 M_\odot$, chosen for consistency with the values of this parameter resulting from the study of the radial velocity curve of the companion (Bassa et al. 2006; Coccoza et al. 2006).

Figure 3 displays in panel (a) the $\Delta\chi^2$ map obtained after calculating the χ^2 values in a 2048×2048 grid for the parameters of our interest. In panels (b) and (c), the posterior probability

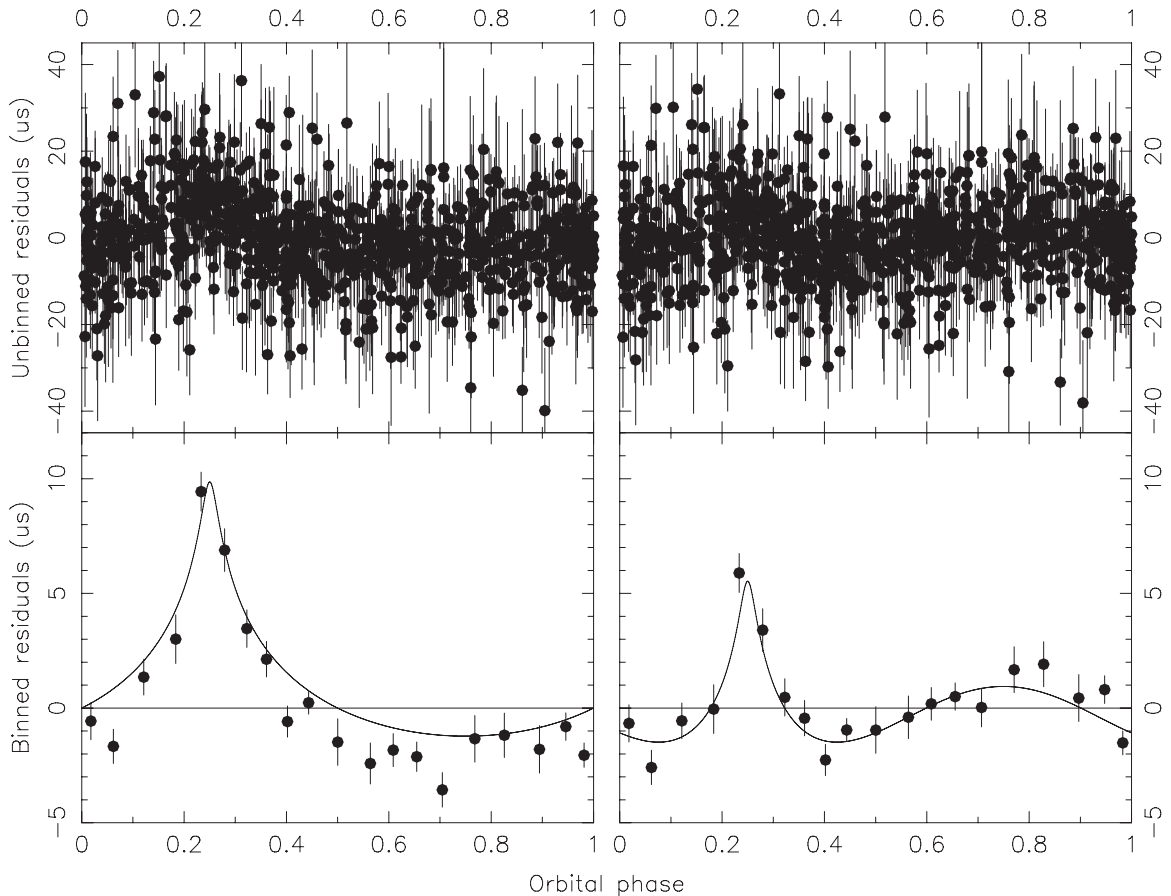


Figure 2. Timing residuals vs. orbital phase. Upper panels display unbinned residuals, while lower panels display residuals after being binned in 20 orbital phase bins. The left panels are related to the attempt of detecting the first harmonic of the Shapiro delay, while the right panels concern the third harmonic. The solid lines in the lower panels are the theoretical curves for the respective harmonics.

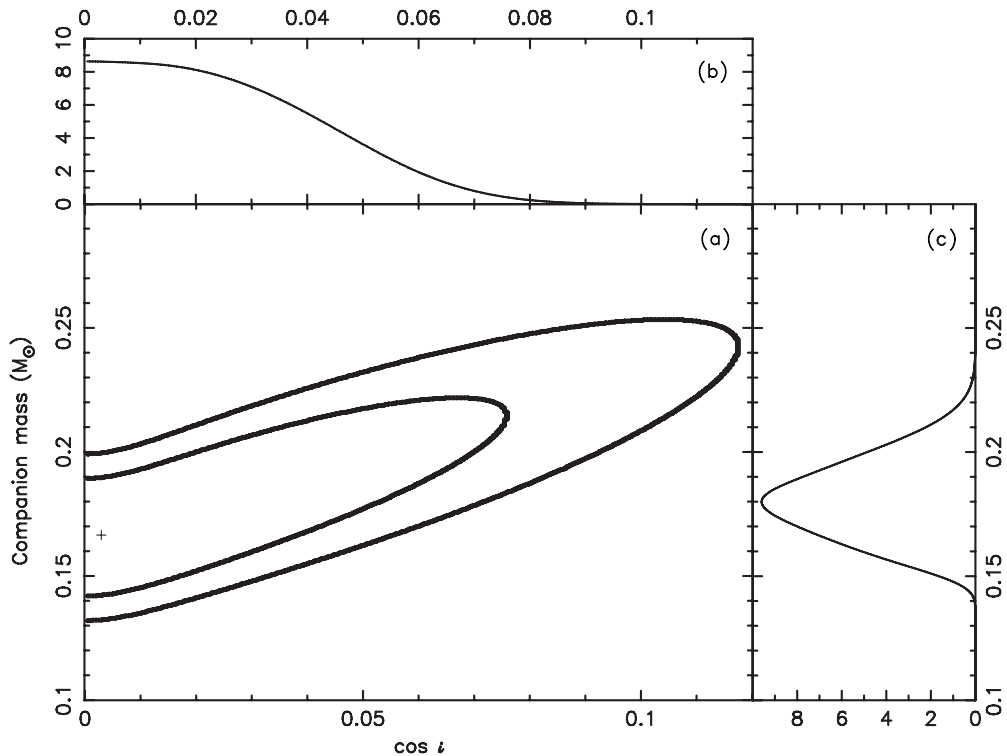


Figure 3. (a) χ^2 map in the $\cos i$ – M_C space. The cross is located at the point of minimum χ^2 . The two solid lines correspond to the 1σ (inner line) and 2σ (outer line) regions. (b) Posterior probability density function for $\cos i$. (c) Posterior probability density function for M_C .

density functions for $\cos i$ and M_C , respectively, are reported. From this analysis, we derived a lower limit for the orbital inclination $\sin i \geq 0.9994$, i.e., $i \geq 88^\circ$ and the value for the companion mass $M_C = 0.180 \pm 0.018 M_\odot$.

3.2. Implications

Under the hypothesis that PSRA is associated with NGC 6752, the measurement reported in Section 3.1 is the second of this kind for a binary pulsar in a globular cluster after PSR J1807–2459B in NGC 6544 (Lynch et al. 2012). PSR J1807–2459B is an MSP with a spin period $P_0 = 4.19$ ms in a highly eccentric orbit $e = 0.747$. The nature of the companion is not yet determined, however, its high mass $M_C = 1.21 M_\odot$ points toward a neutron star or a massive white dwarf (WD) companion. Thus, PSRA represents the first case of a low-mass binary pulsar in a globular cluster for which the Shapiro delay has been detected.

Our determination of the companion mass, $M_C = 0.180 \pm 0.018 M_\odot$, is solely based on the relativistic Shapiro delay and so we did not assume any *a priori* hypothesis on the nature of the companion or the modeling of its structure. In this respect, the full agreement with the values for M_C obtained using observations in the optical band provides independent support to the previously suggested interpretation of the nature of the binary companion of PSRA, i.e., that it is a low-mass helium-core WD (Bassa et al. 2003, 2006; Ferraro et al. 2003; Coccoza et al. 2006). This also gives support to the physical modeling (i.e., the relationship between mass, radius, temperature, and surface gravity of this category of WDs) invoked for deriving the parameters of PSRA from the photometric and spectroscopic data only.

Bassa et al. (2006) attempted to use a comparison between the observed parameters and the models mentioned above in order to decide whether or not this binary system belongs to the globular cluster NGC 6752. Unfortunately, the uncertainties in the measurements of the companion parameters prevented them from drawing a firm conclusion. Since our uncertainty on M_C is similar to that of Bassa et al. (2006), our result does not help in addressing this point. Further support for the association of PSRA with NGC 6752 is expected from the measurement of proper motion for the three isolated pulsars in the core of NGC 6752¹⁰ and comparison with the already accurately determined proper motion for PSRA (Paper II).

Assuming that PSRA is associated with NGC 6752, the timing determination of the companion mass opens the possibility of using the system for testing the various theoretical mass–radius relations proposed for HeWDs. The large uncertainties in the determination of the masses and of the distances of the WDs via optical observations make this difficult. This problem is particularly important for the low-mass WDs, for which accurate determinations of the mass and the radius are rare. In this case, we have independent measurements for the mass of the companion of PSRA and its distance, which is equal to the cluster’s one under our hypothesis. From optical data, Bassa et al. (2006) derive a companion radius, namely, $R_C = 0.058 \pm 0.004 R_\odot$ if PSRA belongs to NGC 6752. We note that the mass–radius relations predicted by both the models of Rohrmann et al. (2002) and Serenelli et al. (2002) nicely agree with the case of a WD of $R_C = 0.058 \pm 0.004 R_\odot$ and $M_C = 0.180 \pm 0.018 M_\odot$. The two models differ in the progenitor’s metallicity, namely, the Rohrmann et al. (2002) model describes low-mass WDs with solar metallicity while the Serenelli et al. (2002) model is suitable for metallicities comparable to the one of NGC 6752. The model by Driebe et al. (1998) computes the WD radius only for masses $M_{\text{WD}} \geq 0.180 M_\odot$. It cannot yet be discarded (for reference, see Figure 6 in Bassa et al. 2006).

Given a typical $\sim 8\%$ uncertainty in the radius determination from optical observations, in order to discriminate between various models for the mass–radius relations, an uncertainty on M_C of $0.002 M_\odot$ is typically required. Unfortunately, several decades are required to achieve this goal with a 64 m class telescope; such high precision could be obtained in about one decade by observing PSRA with the Square Kilometer Array.

A determination of the mass M_P for PSRA can be obtained from our Shapiro delay measurement. From the lower limit in the orbital inclination and the pulsar mass function, we can obtain a firm range for M_P , $1.1 M_\odot \leq M_P \leq 1.5 M_\odot$, from which we deduce the total mass for the system lying in the range $1.26 M_\odot \leq M_{\text{tot}} \leq 1.70 M_\odot$. If we instead use the mass ratio determined by combining the pulsar mass function from pulsar timing and the companion’s mass function from the studies on the companion’s velocity curve by Bassa et al. (2006) and Coccoza et al. (2006), we can slightly improve our results. Bassa et al. (2006) report $M_P/M_C = 7.36 \pm 0.25$, from which we now obtain $M_{\text{tot}} = 1.50 \pm 0.14 M_\odot$ and $M_P = 1.32 \pm 0.14 M_\odot$, while Coccoza et al. (2006) report $M_P/M_C = 7.49 \pm 0.68$, from which we now obtain $M_{\text{tot}} = 1.53 \pm 0.18 M_\odot$ and $M_P = 1.35 \pm 0.18 M_\odot$. The weighted average of these two values yields $M_P = 1.33 \pm 0.11 M_\odot$.

It is worth mentioning that the value for the mass of PSRA is close to the lower edge of the mass range for binary MSPs located in the Galactic disk whose companion is a HeWD star. Since in these systems the neutron star has experienced only one recycling phase, thus leaving the original neutron star mass almost unchanged, the value for the mass of PSRA suggests that this pulsar underwent only one recycling stage. If we combine this statement with the hypothesis that PSRA belongs to the cluster, we can speculate that the ejection of this system toward the cluster’s outskirts (Colpi et al. 2002, 2003) most likely happened in an early stage of the cluster evolution, preventing this binary from experiencing further exchange interactions with the stars in the crowded environment of the cluster’s core. This appears to be at odds with the predictions of the models which suggest that the ejection occurred in the last ~ 1 Gyr (Colpi et al. 2002).

4. CORRELATIONS AMONG THE ORBITAL PERIOD, THE PULSAR, AND THE COMPANION MASS FOR LOW-MASS BINARY PULSARS

TS99 presented detailed numerical calculations on the non-conservative evolution of close binary systems with a low-mass ($M_D < 2.0 M_\odot$) donor star, a $1.3 M_\odot$ accreting neutron star, and an orbital period $P_B \geq 2$ days at the beginning of the LMXB phase. The evolution of LMXBs has already been modeled by Pylyser & Savonije (1988, 1989), who predict that binaries with starting periods $P_B \geq P_{\text{bif}} \simeq 2$ days increase their orbital separation, hence their orbital period, during the mass transfer (diverging systems), while the ones with $P_B \leq P_{\text{bif}}$ decrease their orbital separation (converging systems). In this second case, a simple argument shows that the binary period decreases if $|M_{\text{tot}}|/M_{\text{tot}} < |\dot{a}|/a$ and increases if $|M_{\text{tot}}|/M_{\text{tot}} > |\dot{a}|/a$, where M_{tot} is the total mass of the binary and a is its orbital separation.

¹⁰ They certainly belong to NGC 6752 since at least two of them show the large $|\dot{P}|$ attributed to the gravitational pull of the cluster. Their proper motion has not yet been measured since they are weaker sources.

Table 2
Masses for Binary Pulsars with a Low-mass White Dwarf Companion

PSR	Pulsar Mass (M_{\odot})	Companion Mass (M_{\odot})	Orbital Period (days)	Method	Reference
J0437-4715	1.76 ± 0.20	0.254 ± 0.014	5.74	r,s	Verbiest et al. (2008)
J0751+1807	1.26 ± 0.14	0.191 ± 0.015	0.26	r,s	Nice et al. (2008)
J1012+5307 ^a	1.6 ± 0.2	0.16 ± 0.02	0.60	optical	van Kerkwijk et al. (2005)
J1012+5307 ^a	1.9 ± 0.2	0.16 ± 0.02	0.60	optical	van Kerkwijk et al. (2005)
J1713+0747	1.3 ± 0.2	0.28 ± 0.03	67.83	r,s	Splaver et al. (2005)
J1853+1303	1.4 ± 0.7	$0.33-0.37$	115.65	TS99	Gonzalez et al. (2011)
B1855+09	1.6 ± 0.2	0.270 ± 0.025	12.33	r,s	Splaver (2004)
J1909-3744	1.438 ± 0.024	0.2038 ± 0.0022	1.53	r,s	Jacoby et al. (2005)
J1910+1256	1.6 ± 0.6	$0.30-0.34$	58.47	TS99	Gonzalez et al. (2011)
J1910-5959A	1.33 ± 0.11	0.180 ± 0.018	0.84	r,s	this work
B1957+20	2.40 ± 0.12	0.035 ± 0.002	0.38	optical	van Kerkwijk et al. (2011)
J2016+1948	1.0 ± 0.5	$0.43-0.47$	635.04	TS99	Gonzalez et al. (2011)
J1738+0333	1.47 ± 0.06	0.181 ± 0.006	0.35	optical	Antoniadis et al. (2012)

Notes. Uncertainties are at the 1σ level. Pulsars are listed in right ascension order. In the column “Method,” “r,s” means that the masses have been measured by detecting the Shapiro delay, “optical” by analyzing optical observations of the companion, and TS99 by using the numerical results by Tauris & Savonije (1999). Orbital periods have been obtained by browsing the PSRCAT pulsar catalog (<http://www.atnf.csiro.au/research/pulsar/psrcat>, Manchester et al. 2005), and they have been rounded to the second decimal digit since their uncertainties are so small that they can be considered negligible in the discussion in Section 4.

^a See footnote 11.

TS99 focused their attention on diverging LMXBs and they obtain a positive correlation between the orbital period and the final mass of the HeWD companion, i.e., its mass increases with the observed orbital period, and a negative correlation between the orbital period and the mass of the pulsar. In order to compare the theoretical results of TS99 to the observed systems, we searched the literature for low-mass binary pulsars for which a reliable measurement of both the pulsar and the companion mass has been obtained. These values are reported in Table 2 jointly with the binary period and the method used to obtain the masses.

The masses of the two orbiting objects have been determined using Shapiro delay for 6 binaries out of the 12 reported in Table 2 (indicated with the label “r,s”). As we already discussed in Section 3.2, this kind of measurement does not need any a priori hypothesis, hence these six objects can be used to perform six firm and independent tests on the proposed models. The masses for the remaining objects have been determined as follows.

1. *PSR J1012+5307* (van Kerkwijk et al. 2005) *PSR 1738+0333* (Antoniadis et al. 2012) and *PSR B1957+20* (van Kerkwijk et al. 2011). The binary companion has been observed in phase-resolved spectroscopy observations in the optical band. This observing mode leads to the determination of the companion mass function. Pulsar timing gives the pulsar mass function and the knowledge of these two quantities leads to the determination of the mass ratio of the system. The companion mass has been determined by comparing the observed spectroscopic properties to theoretical models for the atmosphere of HeWDs.
2. *PSRs J1853+1303, J1910+1256, and J2016+1948* (Gonzalez et al. 2011). The timing analysis gives a measurement of the proper motion and of the first derivative of the pulsar projected semimajor axis ($d(a_p \sin i)/dt$). This second quantity changes because of the changing orbital inclination due to proper motion (Kopeikin 1996; Arzoumanian et al. 1996). Since this also depends on the unknown angle between the ascending node and proper motion directions, the most probable orbital inclination

has been determined using Monte Carlo simulations. The companion mass is assumed to be that predicted by the TS99 calculation, while the pulsar mass has been obtained by combining the companion mass with the statistically determined orbital inclination and the pulsar mass function.

In Figure 4, we plot the logarithm of the binary period versus companion mass (upper panels) and the pulsar mass (lower panels). We plotted all objects reported in Table 2 in the left panels, while in the right ones we only show those binaries for which the masses have been determined from measured Shapiro delays. We marked with a triangle the position of PSRA in these plots to distinguish it from the field systems which are denoted by diamonds.

In the left upper panel of Figure 4, the solid, dashed, and dotted lines represent the predictions of the $M_C - P_B$ correlation by TS99 (Equations (20) and (21)). With the exception of the squared point in the left bottom part of the plot, all other points well agree with the theoretical lines by TS99. Intriguingly, the extrapolations of the results of TS99 to binary periods lower than 2 days are also in agreement with the observations of binaries with $P_B \leq 2$ days, i.e., systems whose progenitors were converging LMXBs. This means that the hypothesis assumed by TS99 to model the diverging LMXBs can predict rather well the final HeWD mass also for converging systems. The three points highlighted by a diamond shape represent the binaries for which the companion mass was obtained from one of the TS99 models (Gonzalez et al. 2011), so of course they fall on that line in the $M_C - P_B$ plot. The squared point represents the position of PSR B1957+20, a black widow system. For this latter system, we cannot compare the current companion mass with the predictions by TS99 because of the mass loss the companion underwent after the formation of the MSP+WD system. Nevertheless, for the binary period of this system, TS99 predicts a companion mass $\sim 0.18 M_{\odot}$, i.e., higher than the observed one. This is consistent with the hypothesis that this system obeyed the TS99 $M_C - P_B$ correlation at the epoch of the formation of the MSP+WD binary.

We note that the overall agreement of the predicted $M_C - P_B$ correlation with the available measurements has already been

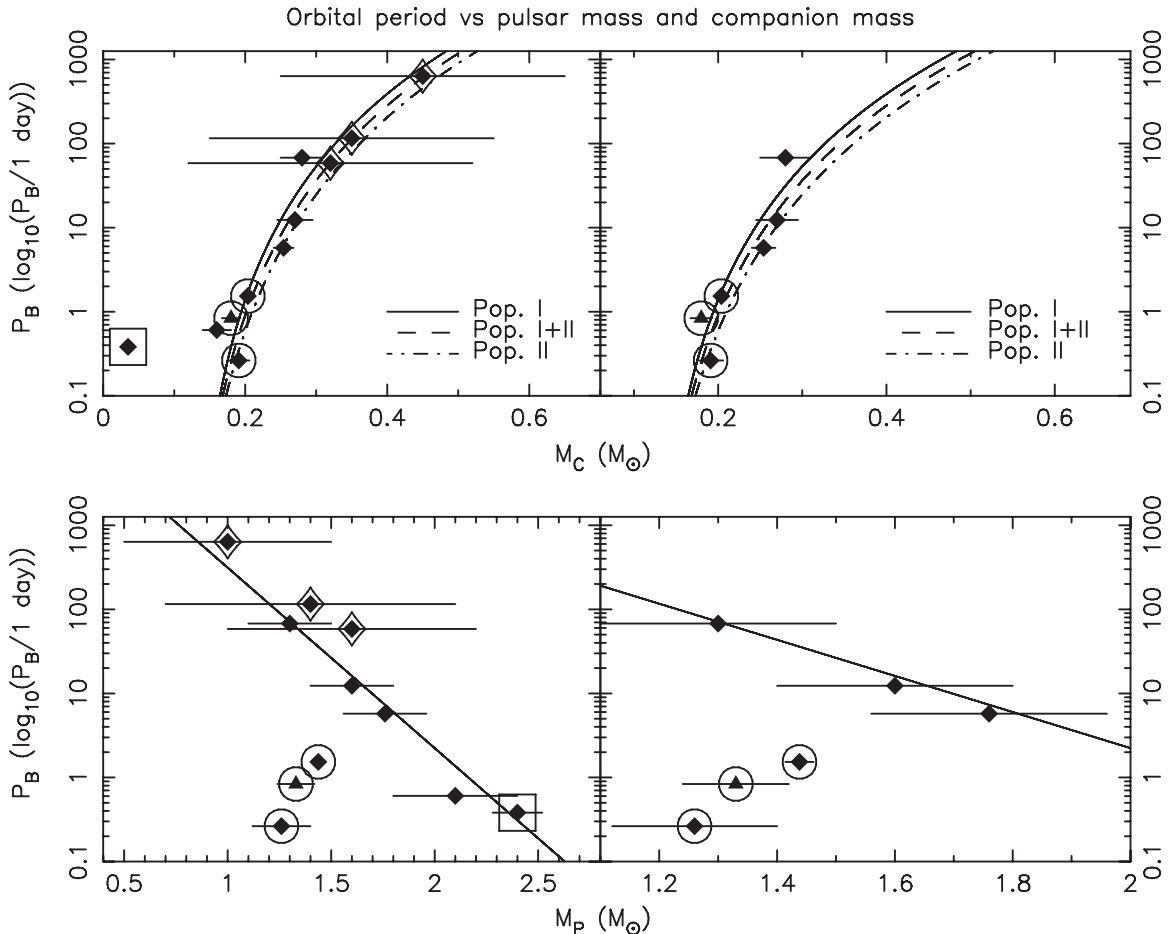


Figure 4. Orbital period vs. companion mass (upper panels) and pulsar mass (lower panels) plots. The left panels show the points related to all binaries in Table 2, while the right panels show the points that represent the binary systems for which the masses have been determined by detecting the Shapiro delay effect only. Error bars are 1σ uncertainties in the masses. If not visible, their size is smaller than the symbol. In all panels, the triangle represents PSRA (the only globular cluster object), diamonds represent field objects, the point enclosed by a square represents PSR B1957+20, the points enclosed by a diamond represent the three objects for which the determination of the companion mass is based on a model by TS99, and the circled points indicate the binaries that do not obey the linear in $\log M_P - P_B$ correlation (the solid line in the bottom plots). In the upper panels the solid, dashed, and dotted lines represent the numerical results by TS99 (Figure 4 in TS99 and the text for details), while in the lower panels the solid lines represent our fit to all plotted points in the bottom left panel except the circled ones.

discussed by various authors (e.g., van Kerkwijk et al. 2005; Lorimer 2008). However, these comparisons were based on a variety of (often) indirect methods for determining M_C , in many cases with rather large confidence intervals for the value for M_C . In the upper right panel of Figure 4, we display a test for the $M_C - P_B$ correlation entirely based on measures obtained via the detection of the Shapiro delay. The theoretical models for the $M_C - P_B$ correlation by TS99 result in agreement to all six test binaries of our sample, including PSRA, the only binary likely associated with a globular cluster.

In the lower left plot of Figure 4, 8 of 11¹¹ objects show a linear correlation between M_P and P_B , while the remaining 4, highlighted with a circle, form a separate group. A comparison between this panel and Figure 4(b) in TS99 indicates that the theoretical predictions overestimate by about $0.5 M_\odot$ the pulsar mass for a given orbital period in the entire range considered by TS99. If a real correlation exists between M_P and P_B for this class of binaries, it is not the one predicted by TS99 as

these authors already pointed out in their comparison with the observed systems.¹²

The solid line is a fit for all plotted points but the circled ones modeling the $M_P - P_B$ correlation by using the following function:

$$\frac{M_P}{M_\odot} = A + B \log_{10} \left(\frac{P_B}{1 \text{ day}} \right) \quad (1)$$

and we obtain $A = 2.180 \pm 0.005$ and $B = -0.475 \pm 0.002$ ($\chi^2 = 0.58$ with 5 degrees of freedom).

In the bottom right panel of Figure 4, the six binaries which represent our firm tests for TS99 are equally divided into two groups: three of them obey the $M_P - P_B$ correlation mentioned above, while the other three do not. The binaries in this second group also have binary periods lower than the bifurcation period $P_{\text{bif}} \simeq 2$ days theoretically found by Pylyser & Savonije (1988, 1989), hence their progenitors were converging LMXBs, while the other three have binary periods higher than P_{bif} , so it is more likely that their progenitors were diverging LMXBs.

The quantitative discrepancy between the TS99 predictions and the observed systems in the $M_P - P_B$ diagram, combined

¹¹ PSR J1012+5307 is excluded from the $M_P - P_B$ plot: two independent measurements for the masses in this binary system are available in the literature (van Kerkwijk et al. 2005 and references therein), agreeing on M_C but not M_P . A firm determination of the pulsar mass is not achieved yet, whence our choice to exclude this object from the $M_P - P_B$ plot and discussion.

¹² The fact that the three objects in Gonzalez et al. (2011) obey the observed $M_P - P_B$ correlation can be seen as an indirect test of the results in TS99 for the $M_C - P_B$ correlation, since the predictions by TS99 have been used only to obtain the companion mass.

with the agreement in the $M_C - P_B$ diagram, indicates that in TS99 the amount of mass released by the companion is well predicted, but the amount of matter captured by the neutron star is overestimated. This means that the discrepancies between the theoretical and observed $M_P - P_B$ diagrams result from an incorrect modeling by TS99 of the mechanisms (one or more) that prevent the neutron star from capturing all the matter released by its companion and are responsible for the mass loss that the binary system undergoes in its LMXB phase. Two mechanisms have been proposed, namely, the radio ejection model (Burderi et al. 2001) and the propeller model (Tauris 2012). Since our test binaries divide themselves in two separate groups, which in turn should have experienced different evolutionary paths for their LMXB progenitors, it is tempting to suggest that the mechanism responsible for the unaccreted matter is different in the two cases of converging and diverging LMXBs, or that in one case only one mechanism takes place at some point of the evolution, while in the other case both mechanisms play a non-negligible role.

The position in the $M_P - P_B$ plot (bottom left) of PSR B1957+20 is apparently at odds with this picture. Its orbital period indicates that its progenitor was a converging LMXB, but it agrees with the possible $M_P - P_B$ correlation for binaries whose progenitors were diverging LMXBs. A first possibility is that the pulsar mass in this system is overestimated. In fact, as reported above, M_P was obtained using indirect methods relying on modeling of the outer layers of the companion star. If the values for M_P of PSR B1957+20 is confirmed by future observations, we could speculate that the family of converging LMXBs must be in turn subdivided in two groups. For the first group, the mechanism(s) preventing the accretion of mass are similar to the diverging systems and the resulting HeWD–MSP binaries obey the same $M_P - P_B$ correlation. The second group is instead characterized by peculiar conditions that make the loss of matter from the binary more efficient. Detailed numerical simulations are required to clarify this point.

5. SUMMARY

In this work, we have presented a timing solution for the binary MSP PSR J1910–5959A based on Parkes timing data with a data span of 12 years. Our new solution gives improved values for the astrometric and rotational parameters compared to those reported in Papers I and II, and contains a new description of the orbital motion including the first detection of the relativistic Shapiro delay for a low-mass MSP in a globular cluster. The measurement of this effect allowed us to determine reliable masses for the two orbiting stars. We have compared the values for the mass and the radius of the companion to the theoretical mass–radius relationships obtained for different chemical compositions, but the current uncertainties on these parameters prevent us from firmly establishing whether PSR J1910–5959A belongs to NGC 6752 or not. Finally, we compared the numerical results on the evolution of LMXB systems obtained by TS99, which predict the presence of a correlation between M_C and P_B and between M_P and P_B for binary systems where an MSP orbits a low-mass HeWD companion, to the sample of these objects for which the masses of the two stars have been measured using Shapiro delay. Observations confirm the $M_C - P_B$ correlation obtained by TS99 and show a possible $M_P - P_B$ correlation for a subset of the sample which is different to the one obtained by TS99. The numerical calculations by these authors overestimate the pulsar mass by about $0.5 M_\odot$. These results confirm that the amount of mass lost by the binary during the evolu-

tion in LMXB is always larger than predicted by TS99. Moreover, they suggest that the low-mass binary pulsars with a WD companion can be split in two groups, characterized by significantly different efficiencies in the mechanisms responsible for the loss of matter during their evolution in the LMXB phase.

A.C., A.P., and N.D. acknowledge support for this research provided by INAF, under the National Research Grant PRIN-INAF 2010, awarded with DP 28/2011. The Parkes radio telescope is part of the Australia Telescope, which is funded by the Commonwealth of Australia for operation as a National Facility managed by CSIRO. We thank the colleagues who assisted with the observations discussed in this paper.

REFERENCES

- Antoniadis, J., van Kerkwijk, M. H., Koester, D., et al. 2012, *MNRAS*, **423**, 3316
- Arzoumanian, Z., Joshi, K., Rasio, F., & Thorsett, S. E. 1996, in ASP Conf. Ser. 105, IAU Colloquium 160, Pulsars: Problems and Progress, ed. S. Johnston, M. A. Walker, & M. Bailes (San Francisco, CA: ASP), **525**
- Bassa, C. G., van Kerkwijk, M. H., Koester, D., & Verbunt, F. 2006, *A&A*, **456**, 295
- Bassa, C. G., Verbunt, F., van Kerkwijk, M. H., & Homer, L. 2003, *A&A*, **409**, L31
- Bhattacharya, D., & van den Heuvel, E. P. J. 1991, *Phys. Rep.*, **203**, 1
- Burderi, L., Possenti, A., D’Antona, F., et al. 2001, *ApJ*, **560**, L71
- Cocozza, G., Ferraro, F. R., Possenti, A., & D’Amico, N. 2006, *ApJ*, **641**, L129
- Colpi, M., Mapelli, M., & Possenti, A. 2003, *ApJ*, **599**, 1260
- Colpi, M., Possenti, A., & Gualandris, A. 2002, *ApJ*, **570**, L85
- Corongiu, A., Possenti, A., Lyne, A. G., et al. 2006, *ApJ*, **653**, 1417
- D’Amico, N., Lyne, A. G., Manchester, R. N., Possenti, A., & Camilo, F. 2001, *ApJ*, **548**, L171
- Damour, T., & Deruelle, N. 1985, Ann. Inst. H. Poincaré (Phys. Théorique), **43**, 107
- Damour, T., & Deruelle, N. 1986, Ann. Inst. H. Poincaré (Phys. Théorique), **44**, 263
- Driebe, T., Schoenberner, D., Bloecker, T., & Herwig, F. 1998, *A&A*, **339**, 123
- Ferraro, F. R., Possenti, A., Sabbi, E., et al. 2003, *ApJ*, **595**, 179
- Gonzalez, M. E., Stairs, I. H., Ferdman, R. D., et al. 2011, *ApJ*, **743**, 102
- Hobbs, G. B., Edwards, R. T., & Manchester, R. N. 2006, *MNRAS*, **369**, 655
- Jacoby, B. A., Hotan, A., Bailes, M., Ord, S., & Kulkarni, S. R. 2005, *ApJ*, **629**, L113
- Kopeikin, S. M. 1996, *ApJ*, **467**, L93
- Lange, C., Camilo, F., Wex, N., et al. 2001, *MNRAS*, **326**, 274
- Lorimer, D. R. 2008, *Living Rev. Relativ.*, **11**, 8
- Lorimer, D. R., & Kramer, M. 2004, *Handbook of Pulsar Astronomy* (Cambridge: Cambridge Univ. Press)
- Lynch, R. S., Freire, P. C. C., Ransom, S. M., & Jacoby, B. A. 2012, *ApJ*, **745**, 109
- Manchester, R. N., Hobbs, G. B., Teoh, A., & Hobbs, M. 2005, *AJ*, **129**, 1993
- Nice, D. J., Stairs, I. H., & Kasian, L. E. 2008, in AIP Conf. Proc. 983, 40 Years of Pulsars: Millisecond Pulsars, Magnetars and More, ed. C. Bassa, Z. Wang, A. Cumming, & V. M. Kaspi (Melville, NY: AIP), **453**
- Polymer, E., & Savonije, G. J. 1988, *A&A*, **191**, 57
- Polymer, E., & Savonije, G. J. 1989, *A&A*, **208**, 52
- Rohrmann, R. D., Serenelli, A. M., Althaus, L. G., & Benvenuto, O. G. 2002, *MNRAS*, **335**, 499
- Serenelli, A. M., Althaus, L. G., Rohrmann, R. D., & Benvenuto, O. G. 2002, *MNRAS*, **337**, 1091
- Splaver, E. M. 2004, PhD thesis, Princeton Univ.
- Splaver, E. M., Nice, D. J., Arzoumanian, Z., et al. 2002, *ApJ*, **581**, 509
- Splaver, E. M., Nice, D. J., Stairs, I. H., Lommen, A. N., & Backer, D. C. 2005, *ApJ*, **620**, 405
- Staveley-Smith, L., Wilson, W. E., Bird, T. S., et al. 1996, *PASA*, **13**, 243
- Tauris, T. M. 2012, *Science*, **335**, 561
- Tauris, T. M., & Savonije, G. J. 1999, *A&A*, **350**, 928
- van Kerkwijk, M., Bassa, C. G., Jacoby, B. A., & Jonker, P. G. 2005, in ASP Conf. Ser. 328, *Binary Radio Pulsars*, ed. F. Rasio & I. H. Stairs (San Francisco, CA: ASP), **357**
- van Kerkwijk, M. H., Breton, R. P., & Kulkarni, S. R. 2011, *ApJ*, **728**, 95
- van Straten, W., & Bailes, M. 2011, *PASA*, **28**, 1
- Verbiest, J. P. W., Bailes, M., van Straten, W., et al. 2008, *ApJ*, **679**, 675

ERRATUM: “A SHAPIRO DELAY DETECTION IN THE BINARY SYSTEM HOSTING THE MILLISECOND PULSAR PSR J1910–5959A” (2012, ApJ, 760, 100)

A. CORONGIU¹, M. BURGAY¹, A. POSSENTI¹, F. CAMILO², N. D’AMICO^{1,3}, A. G. LYNE⁴, R. N. MANCHESTER⁵, J. M. SARKISSIAN⁶, M. BAILES⁷, S. JOHNSTON⁵, M. KRAMER^{4,8}, AND W. VAN STRATEN⁷

¹ INAF - Osservatorio Astronomico di Cagliari, Loc. Poggio dei Pini, Strada 54, I-09012 Capoterra (CA), Italy

² Columbia Astrophysics Laboratory, Columbia University, 550 West, 120th Street, New York, NY 10027, USA

³ Dip. di Fisica, Università degli Studi di Cagliari, S.S. Monserrato-Sestu km 0,700, I-09042 Monserrato (CA), Italy

⁴ Jodrell Bank Centre for Astrophysics, School of Physics and Astronomy, University of Manchester, Manchester M13 9PL, UK

⁵ CSIRO Astronomy and Space Science, Australia Telescope National Facility, P.O. Box 76, Epping, NSW 1710, Australia

⁶ Australia Telescope National Facility, CSIRO, Parkes Observatory, P.O. Box 276, Parkes, NSW 2870, Australia

⁷ Centre for Astrophysics and Supercomputing, Swinburne University of Technology, P.O. Box 218 Hawthorn, VIC 3122, Australia

⁸ Max-Planck-Institut für Radioastronomie, Auf dem Hügel 69, D-53121 Bonn, Germany

Received 2012 December 10; published 2013 January 8

Figure 4 appeared incorrectly in the published version of this article. The correct version of Figure 4 is the one reported here below. The caption is unchanged. The content and the results of the paper are also unchanged.

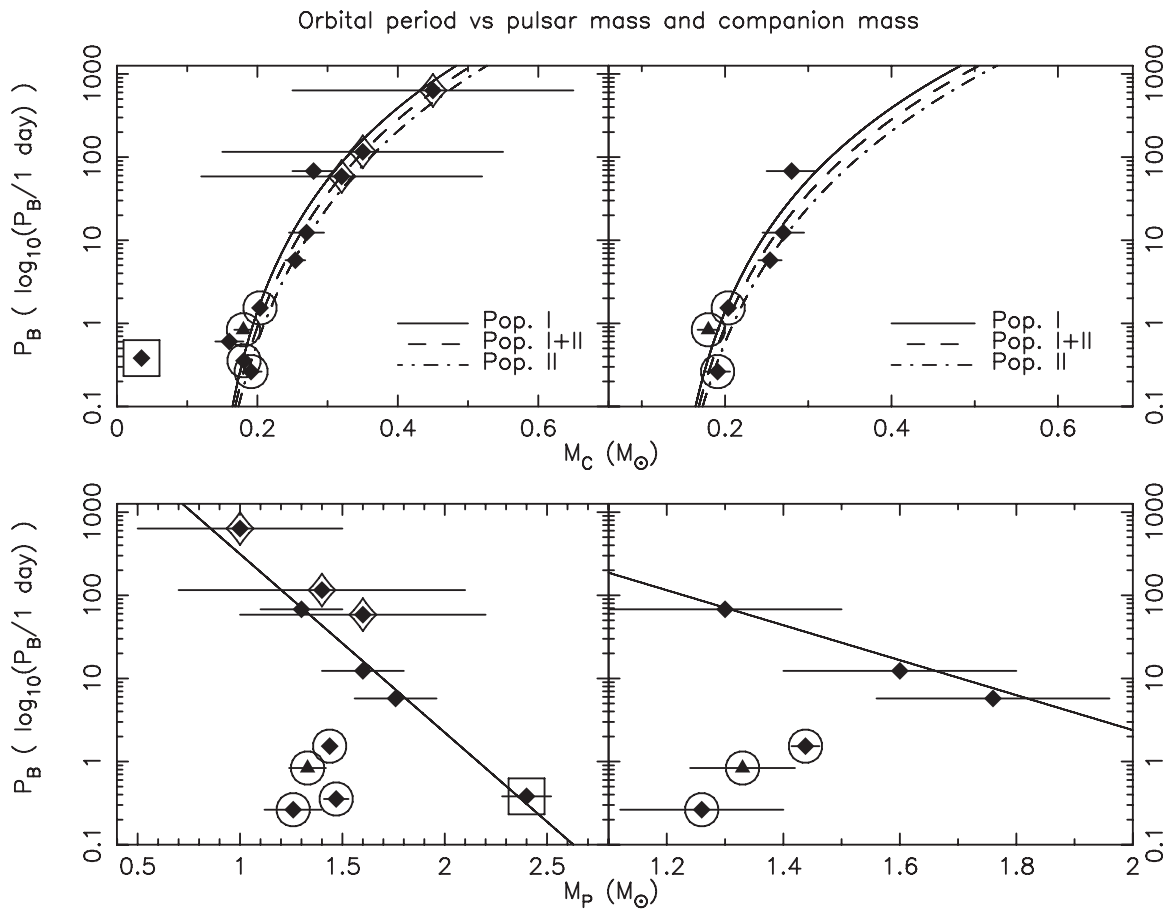


Figure 4.